Evolution of Analog Circuit Models of Ion Channels

Theodore W. Cornforth[1], Kyung-Joong Kim[2], and Hod Lipson[3]

[1] Department of Biological Statistics and Computational Biology, Cornell University, Ithaca, USA 14853
twc63@cornell.edu
[2] Department of Computer Engineering, Sejong University, 98 Gunja-Dong, Gwangjin-Gu, Seoul 143-747, Republic of Korea
kimkj@sejong.ac.kr
[3] Department of Mechanical and Aerospace Engineering, Cornell University, Ithaca, USA 14853
hl274@cornell.edu

Abstract. Analog circuits have long been used to model the electrical properties of biological neurons. For example, the classic Hodgkin-Huxley model represents ion channels embedded in a neuron's cell membrane as a capacitor in parallel with batteries and resistors. However, to match the predictions of the model with their empirical electrophysiological data, Hodgkin and Huxley described the nonlinear resistors using a complex system of coupled differential equations, a celebrated feat that required exceptional creativity and insight. Here, we use evolutionary circuit design to emulate such leaps of human creativity and automatically construct equivalent circuits for neurons. Using only direct electrophysiological observations, the system evolved circuits out of basic electronic components that accurately simulate the behavior of sodium and potassium ion channels. This approach has the potential to serve both as a modeling tool to reverse engineer complex neurophysiological systems and as an assistant in the task of hand-designing neuromorphic circuits.

1 Introduction

At least since the work of Lapicque in 1907 [1,23], analog circuits have been used as models to aid in understanding the behavior of biological neurons. Lapicque had knowledge of empirical observations as shown in Fig. 1. On the basis of such observations, he reasoned that the lipid bilayer membrane separating the intracellular space from the extracellular fluid is capable of storing charge and so acts like a capacitor. In addition, measurements of the membrane voltage in response to applied currents suggested the presence of a 'leak' conductance that acts like a resistor-battery combination in its tendency to slowly return the membrane voltage to a baseline resting value. An analog circuit matching this description is a capacitor in parallel with a resistor and battery, and is perhaps the simplest circuit capable of reproducing the fundamental electrical behavior

G. Tempesti, A.M. Tyrrell, and J.F. Miller (Eds.): ICES 2010, LNCS 6274, pp. 157–168, 2010.

of a neuron (Fig. 2). Such a circuit is usually referred to as an 'equivalent' circuit in that it reproduces the essential behavior of a more complex electrical system in relatively simple form.

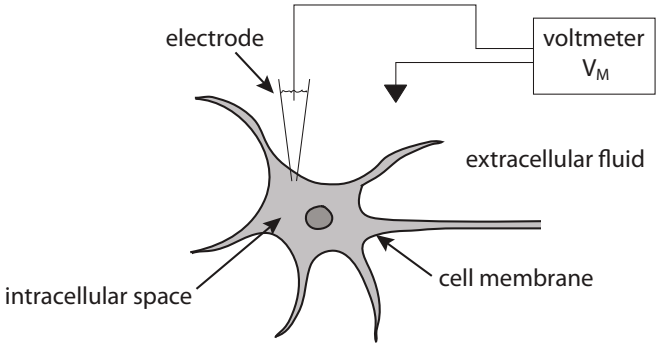

Fig. 1. Simple electrophysiology setup. Using a micromanipulator and microscope, a glass electrode can be positioned inside an individual neuron in such a way as to minimize damage to the cell membrane. This creates a simple circuit for measuring the potential difference between the intracellular space and the extracellular fluid. This potential difference is called the membrane voltage, V_M. A stimulus current (the 'input' to the cell) can be delivered through the electrode and the resulting changes in V_M (the 'output' from the cell) recorded for later study.

The concept of an equivalent circuit for a neuron has proven useful for the development of more sophisticated models of neuron behavior. Lapicque himself used the above circuit as the basis for the widely used integrate-and-fire model, in which all-or-nothing spikes in membrane voltage called action potentials are triggered when the capacitor is charged to some threshold potential [23]. Although useful for many purposes, the integrate-and-fire model does not describe the complex dynamics of the numerous membrane conductances in a typical neuron, of which the above-mentioned leakage conductance is only the simplest.

Today, these different conductances are known to correspond to different types of membrane-spanning pores in the cell membrane called ion channels [10]. Ion channels are characterized by the type of ion that flows through them as well as by the factors that influence the degree to which the channel admits that ion. For example, a voltage-gated sodium channel admits only sodium ions and the intrinsic rate of sodium ion passage through the channel depends on the membrane voltage. The behavior of individual channel types and even individual channel molecules can be studied in isolation through different pharmacological and electromechanical techniques [18].

A major breakthrough in computational neuroscience was the detailed mathematical description of the primary conductances involved in action potential generation by Hodgkin and Huxley, for which they were awarded the 1963 Nobel Prize in Physiology or Medicine [15]. The equivalent circuit used by Hodgkin and

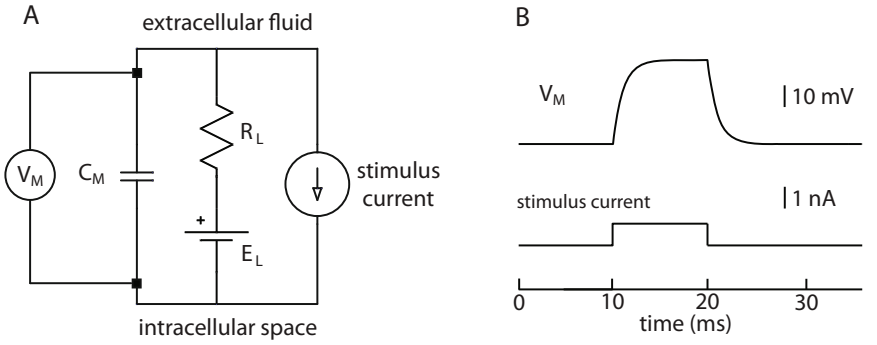

Fig. 2. A. Lapicque's equivalent analog circuit for a neuron. With properly adjusted component parameters, this circuit reproduces the fundamental passive electrical behavior of a neuron. The battery-resistor combination represents the intrinsic driving force on ions comprising the leak current and the resistance to their flow across the membrane. Typical values for the components are on the order of 1 GΩ for the leak resistance (R_L), -70 mV for the leak potential (E_L), 1 pF for membrane capacitance (C_M) and 1 nA for the stimulus current. The node at the top of the circuit represents the extracellular fluid and the node at the bottom represents the intracellular space. A major simplifying assumption in this minimal model is that both the extracellular and intracellular spaces are isopotential compartments. **B.** Just as with a biological neuron, the circuit's membrane voltage (top) in response to small step current inputs (bottom) behaves like the charging and discharging of an RC circuit.

Huxley, with components for sodium and potassium conductances in addition to the leakage conductance, is shown in Fig. 3A. In this case, the behavior of the nonlinear resistors is described by a complex system of coupled differential equations (Fig. 3B). This model is frequently cited as perhaps the most remarkable feat of creativity and insight in all of computational neuroscience, in part because Hodgkin and Huxley were unaware at the time of the correspondence between ion channels and membrane conductances [8].

If artificial intelligence were capable of such extraordinary leaps of creativity and insight in the face of little or no mechanistic understanding of the underlying physiology, it would be a very powerful tool in the neuroscientist's toolbox. Although action potentials are important, they are just one among the hundreds if not thousands of dynamical systems that would need to be modeled to develop a reasonably complete picture of single cell neurophysiology. These include the dynamical systems underlying synaptic transmission, vesicle cycling, axon and dendrite growth, apoptosis and general cell metabolism [18]. This vast undertaking is of great interest not only for purely theoretical reasons, but for biomedical applications that require accurate neurophysiological models [5]. Our goal is to shift much of the burden of creating these models from humans to computers.

Here, we apply the established technique of analog circuit evolution [22] to the task of creating equivalent circuit models for neurophysiological systems. The systems are measured through very simple, direct experiments of the kind that can easily be performed in a typical neuroscience 'wet' lab. With only this

A

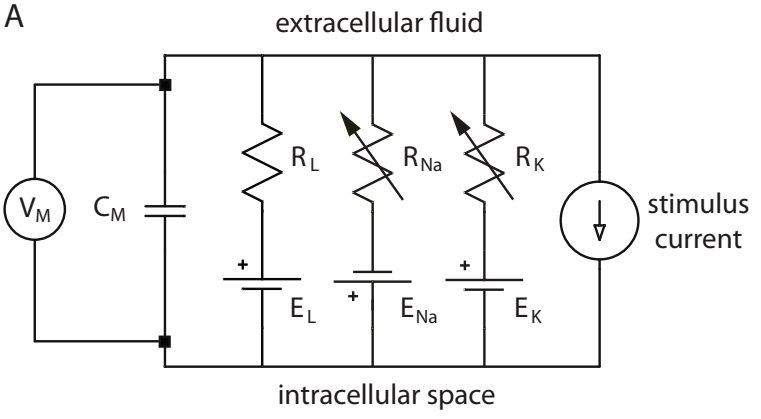

B

$$\frac{dv}{dt} = f(v, h, m, n, i) = -120\, m^3\, h\, (v - 45) - 36\, n^4\, (v + 82) - 0.5\,(v + 60)$$

$$\frac{dh}{dt} = f(v, h) = 0.07\, e^{-\frac{1}{20} v - \frac{7}{2}}\, (1 - h) - \frac{1.0\, h}{1 + e^{-\frac{1}{10} v - 4}}$$

$$\frac{dm}{dt} = f(v, m) = \frac{1}{10}\, \frac{(v + 45)\, (1 - m)}{1 - e^{-\frac{1}{10} v - \frac{9}{2}}} - 4.0\, e^{-\frac{1}{18} v - \frac{35}{9}}\, m$$

$$\frac{dn}{dt} = f(v, n) = \frac{0.1 \left(\frac{1}{10} v + 6 \right) (1 - n)}{1 - e^{-\frac{1}{10} v - 6}} - 0.125\, e^{-\frac{1}{80} v - \frac{7}{8}}\, n$$

Fig. 3. A. The Hodgkin-Huxley equivalent circuit. This circuit is similar to Lapicque's circuit in Fig. 2 except that terms for sodium (R_{Na}, E_{Na}) and potassium (R_K, E_K) conductances have been added. Another significant difference is the nonlinear nature of the R_{Na} and R_K resistors, whose dynamics are described in the system of differential equations in B. **B.** The original Hodgkin-Huxley dynamical system. The variable v corresponds to the observed membrane voltage, the variable i corresponds to the stimulus current, and the hidden variables h, m, n correspond to gating parameters of the sodium and potassium conductances. Although the system is typically not presented in its full form without extensive explanation, we do so here to emphasize the complexity of the task faced by Hodgkin and Huxley and the magnitude of their achievement. For details, see the description in [15] or the accessible introduction in [17].

input data and with only the simplest electrical components such as resistors and capacitors, circuit evolution can automatically generate accurate equivalent circuits for ion channels of the type studied by Hodgkin and Huxley.

2 Methods

2.1 Circuit Evolution

We employ a simple version of Koza's circuit evolution technique [19,22]. Initially, a population of candidate equivalent circuits is created with two randomly selected, randomly connected electrical components. These randomly chosen components are placed in a variable portion of an otherwise invariant embryonic circuit as shown in Fig. 4. The fitness of individuals in this random population is evaluated by translating each individual into an equivalent Spice netlist, simulating its behavior using NGSpice20 [28], and comparing this behavior to that of the target neurophysiological system (see *Neurophysiological Data* below). A steady-state population-updating method is used in which the least fit half of the population is subject to mutation before the next generation of fitness evaluation and selection occurs. For all results reported, no recombination was used and populations had a size of 48.

We represent circuits with a direct schematic-based encoding, in which components and their connections are stored as flat lists [6]. Seven low-level electrical components were used as the raw material or 'building blocks' with which evolution operates. These components and their variable parameter ranges are shown in Appendix A, Table 1. All models are default NGSpice20 models with the exception of the MOSFET models, which were generously provided by Mario Simoni [32]. From each circuit that is chosen to be mutated, one randomly selected component undergoes one of eight possible mutations. For details on these mutation operations, see our previous paper [19]. For some experiments, hill-climbing and random search controls were used. For hill-climbing, each 'generation' consisted of mutating a single circuit and replacing it with the mutated circuit if the mutation improved fitness. Similarly, for each generation in a random search, a circuit was randomly constructed from scratch and used to replace the best previously encountered circuit if the new circuit had higher fitness. For both hill-climbing and random search, the search was continued until the total number of circuits evaluated matched the number evaluated with a corresponding evolutionary procedure.

2.2 Neurophysiological Data

For our initial experiments, we simulated the 1952 Hodgkin-Huxley studies in which the contribution of the primary sodium and potassium currents to the squid giant axon action potential were studied in isolation using pharmacological techniques [12–16]. Using the NEURON 7.0 simulation environment [11], we inserted default HH sodium and potassium channels into a single compartment.

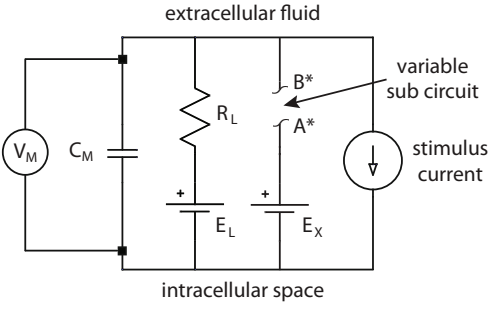

Fig. 4. The embryonic circuit. This circuit is essentially a model of a cell membrane with no ion channels embedded except for those responsible for the leak current. It is the task of evolution to find a sub circuit such that the entire circuit reproduces the behavior of a target ion channel. The nodes labeled A* and B* are used to identify connection points for the evolved sub circuits shown in Fig. 6 and Fig. 7 below. We include the intrinsic driving force for the modeled ion channel (E_X) as this is easy to determine experimentally and is not difficult to model, unlike the portion of the circuit that would be equivalent to the nonlinear resistors in Fig. 3.

Such a simulated 'cell' has the equivalent circuit shown in Fig. 2A. We then set the conductance values for sodium to 0 to simulate pharmacological blockade of the voltage-gated sodium channels and stimulated the cell with a small step current of 1 nA. The membrane voltage response obtained in this way represents the target behavior of idealized voltage-gated potassium ion channels (Fig. 5). In other words, evolution is tasked with finding a variable sub circuit as in Fig. 4 that behaves in the same way as the Hodgkin-Huxley nonlinear potassium resistance R_K. The voltage-gated sodium channel is targeted for evolution in a similar manner.

To evaluate the fitness of a candidate equivalent circuit, we stimulate it with a step current of 1 nA in NGSpice20 and compare the resulting membrane voltage time series with the simulated membrane voltage time series obtained from NEURON (Fig. 5). Spice simulation data is recorded at 0.1 ms resolution for 40 ms and each of those 401 time points are compared with the corresponding time points from the target NEURON data. Fitness is then defined as the reciprocal of the sum of the absolute differences at each time point. To reduce fitting errors due simply to voltage offset or scaling, both of the membrane voltage time series involved in the comparison are normalized to the range 0-1. Results below are plotted on this relative voltage scale.

3 Results

Evolution produced compact circuits mimicking the behavior of both an idealized voltage-gated potassium channel and a voltage-gated sodium channel. Fig. 5A shows the step response of a typical evolved equivalent circuit for the

voltage-gated potassium channel compared with the target potassium channel step response. Fig. 6 is the schematic for this evolved equivalent circuit. Similarly, Fig. 5B shows the response of a typical evolved circuit for the voltage-gated sodium channel and Fig. 7 is the schematic for this evolved equivalent circuit. Performance of the evolutionary algorithm for potassium channel equivalent circuit evolution and sodium channel equivalent circuit evolution are shown in Fig. 8A and Fig. 8B, respectively. Typical runs showed convergence to final fitness values within 1000 evolutionary generations, which requires about 150 minutes on a modest 2GHz quad-core machine.

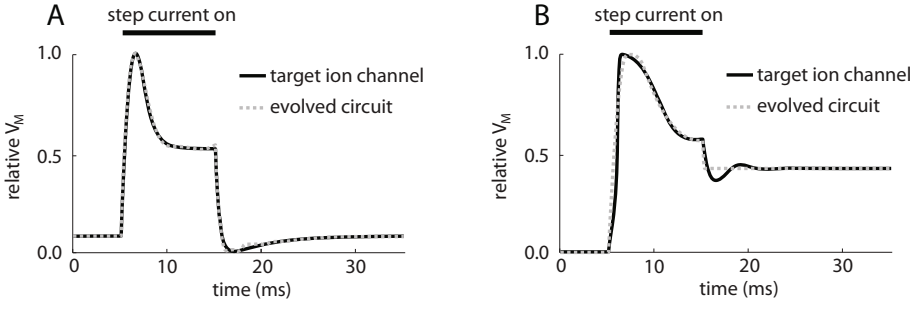

Fig. 5. Step response of the voltage-gated potassium (A) and sodium (B) channels (c.f. Fig. 2B). The responses of idealized NEURON ion channels to a step current of 1 nA are shown with solid black lines and the responses of embryonic circuits plus an evolved sub circuit are shown with dashed gray lines.

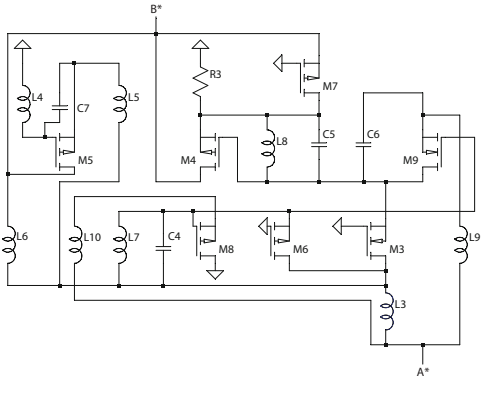

Fig. 6. Schematic of an evolved potassium channel equivalent circuit. No post-processing or simplification of the circuit was performed. To conserve space, only the evolved variable sub circuit is shown. Parameter values are shown in Appendix A, Table 2. The nodes labeled A* and B* connect with the embryonic circuit as shown in Fig. 4.

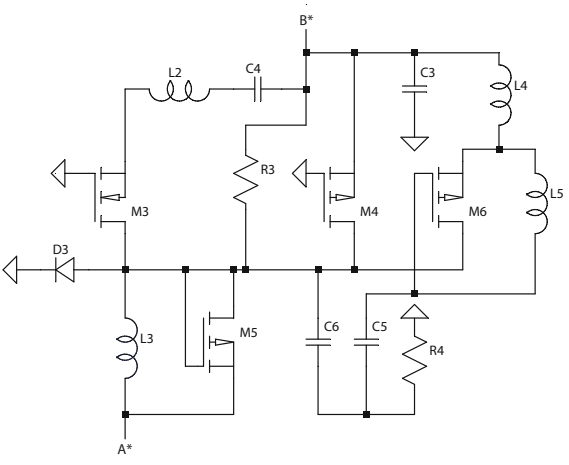

Fig. 7. Schematic of an evolved sodium channel equivalent circuit. As in Fig. 6, only the evolved variable sub circuit is shown and no post-processing or simplification of the circuit was performed. Parameter values are shown in Appendix A, Table 3.

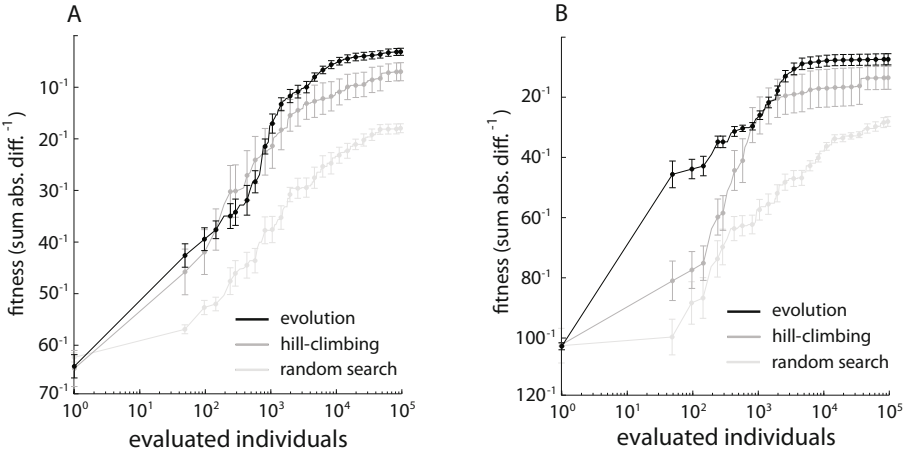

Fig. 8. Equivalent circuit fitness as a function of the number of evaluated individuals. Potassium (A) or sodium (B) channel equivalent circuits were found with evolutionary search (black), hill-climbing (dark gray), and random search (light gray) for ten independent runs each. In each case, fitness was being maximized as described in Methods above. The mean fitness across runs of the best equivalent circuit is plotted as a solid line with error bars representing mean fitness ± standard error of the mean.

4 Discussion and Conclusion

We propose that circuit evolution can be used to automatically construct equivalent circuits for neurophysiological systems. We tested this idea on two systems,

voltage-gated sodium and potassium ion channels, and found that the evolved circuits can reproduce the behavior of the modeled systems to a large degree.

Future work will confirm that the evolved equivalent circuits are accurate and robust models of the sodium and potassium ion channels. The behavior of the evolved sodium channel circuits in particular deviate somewhat from the desired behavior. One possible explanation is that Hodgkin-Huxley voltage-gated sodium channel dynamics involve both activation and inactivation processes, unlike the dynamics of voltage-gated potassium channels, which can be modeled with only activation. We are pursuing the hypothesis that recombination would allow a promising sub circuit for only the activation or only the inactivation process to replicate and then differentiate during evolution. We are also investigating more sophisticated representations for analog circuit evolution such as Analog Genetic Encoding [26] and graph grammar-based approaches [3].

We used step current inputs to the respective systems to characterize their output behavior, but it will be important to confirm that other types of input/output pairings can be reproduced by the equivalent circuits as well. Co-evolution of input functions and equivalent circuit models is one possible way to maintain selection pressure for robustness [35]. Such a co-evolutionary approach was tried in our previous paper [19] with good results. Our longer-term goal is to move beyond ion channels simulated in NEURON and to use circuit evolution as one component of a closed-loop automated experiment system. Active learning would be used to probe a physical system of interest, such as a single neuron as shown in Fig. 1A. The inputs that cause the most disagreement between predicted and observed outputs would be used to evolve equivalent circuits. The accuracy and robustness of the model could then be refined by further cycles of active learning probes and circuit evolution. This approach is proposed and discussed in detail in Bongard and Lipson (2007) [2].

The use of circuit evolution to model neurophysiological systems has potential applications beyond those presented here. For example, the design of neuromorphic circuits that interface living tissue with electrical components is of growing importance in the medical field, yet as with the design of all novel analog circuits, neuromorphic circuit design is largely performed by hand and then only by experienced electrical engineers [4,33]. The complexity of hand-designed hardware implementations of the Hodgkin Huxley model attests to the difficulty of the task [21, 32]. The assistance of circuit evolution could be invaluable, especially as neuromorphic circuits customized to the needs of individual patients become a reality [31]. Although we use discrete components here, our approach is applicable to the design of integrated circuits, which would almost certainly be used in any practical neuromorphic system. One drawback of the equivalent circuit approach in general is the lack of a mechanistic correspondence to the underlying neurophysiological system. However, many applications may not require an understanding of the underlying biology in detail. For example, simulations used in drug design might benefit from an accurate and easily-produced model of a neurophysiological system with only the requirement that certain observed behavior be reproduced [29].

Given the inherently electrical nature of systems in neurophysiology, the electrical components in equivalent circuits are likely to be natural building blocks with which evolution can construct accurate models. However, equivalent circuits are only one of many ways to represent neurophysiological systems. Others include differential equations as in Hodgkin and Huxley's work, Markov kinetic models [9] and artificial neural networks [25]. Evolution-based search has now been successfully applied to the optimization of models using all those representations [7, 27, 34]. The more general idea of using software and hardware-based techniques to automatically study systems in biology, chemistry and physics has also had noteworthy successes [20, 24, 30]. Indeed, we envision that many non-trivial scientific tasks currently requiring significant human effort will begin to be augmented by sophisticated artificial intelligence and robotic systems in the near future.

Acknowledgments. Support was provided by the Tri-Institutional Training Program in Computational Biology and Medicine.

References

1. Abbott, L.F.: Lapicque's Introduction of the Integrate-and-Fire Model Neuron. Brain Res. Bull. 50, 303–304 (1999)
2. Bongard, J., Lipson, H.: Automated Reverse Engineering of Nonlinear Dynamical Systems. PNAS 104, 9943–9948 (2007)
3. Das, A., Vemuri, R.: A Graph Grammar Based Approach to Automated Multi-Objective Analog Circuit Design. In: Proc. Design, Automation, Test Eur. Conf., pp. 700–705 (2009)
4. Douglas, R., Mahowald, M., Mead, C.: Neuromorphic Analog VLSI. Ann. Rev. Neurosci. 18, 255–281 (1995)
5. Ellner, S.P., Guckenheimer, J.: Dynamic Models in Biology. Princeton University Press, Princeton (2006)
6. Floreano, D., Mattiussi, C.: Bio-Inspired Artificial Intelligence: Theories, Methods, and Technologies. MIT Press, Cambridge (2008)
7. Gurkiewicz, M., Korngreen, A.: A Numerical Approach to Ion Channel Modeling Using Whole-cell Voltage-clamp Recordings and a Genetic Algorithm. PLOS Comp. Biol. 3, 1633–1647 (2007)
8. Häusser, M.: The Hodgkin-Huxley Theory of the Action Potential. Nat. Neurosci. 3, 1165 (2000)
9. Hawkes, A.G.: Stochastic Modeling of Single Ion Channels. In: Feng, J. (ed.) Computational Neuroscience: a Comprehensive Approach. CRC Press, London (2003)
10. Hille, B.: Ion Channels of Excitable Membranes. Sinauer Associates, Sunderland (2001)
11. Hines, M.L., Carnevale, N.T.: NEURON: a Tool for Neuroscientists. The Neuroscientist 7, 123–135 (2001)
12. Hodgkin, A.L., Huxley, A.F.: Currents Carried by Sodium and Potassium Ions Through the Membrane of the Giant Axon of Loligo. J. Phys. 116, 449–472 (1952)
13. Hodgkin, A.L., Huxley, A.F.: The Components of Membrane Conductance in the Giant Axon of Loligo. J. Phys. 116, 473–496 (1952)

14. Hodgkin, A.L., Huxley, A.F.: The Dual Effect of Membrane Potential on Sodium Conductance in the Giant Axon of Loligo. J. Phys. 116, 497–506 (1952)
15. Hodgkin, A.L., Huxley, A.F.: A quantitative description of Membrane Current and its Application to Conduction and Excitation in Nerve. J. Phys. 117, 500–544 (1952)
16. Hodgkin, A.L., Huxley, A.F., Katz, B.: Measurement of Current-Voltage Relations in the Membrane of the Giant Axon of Loligo. J. Phys. 116, 424–448 (1952)
17. Hoppensteadt, F.C., Peskin, C.S.: Modeling and Simulation in Medicine and the Life Sciences. Springer, New York (2002)
18. Kandel, E.R., Schwartz, J.H., Jessell, T.M.: Principles of Neural Science. McGraw-Hill, New York (2000)
19. Kim, K.-J., Wong, A., Lipson, H.: Automated synthesis of resilient and tamper-evident analog circuits without a single point of failure. Genet. Program. Evolvable Mach. 11, 35–59 (2010)
20. King, R.D., Rowland, J., Oliver, S.G., Young, M., Aubrey, W., Byrne, E., Liakata, M., Markham, M., Pir, P., Soldatova, L.N., Sparkes, A., Whelan, K.E., Clare1, A.: The Automation of Science. Science 324, 85–89 (2009)
21. Kohno, T., Aihara, K.: Bottom-Up Design of Class 2 Silicon Nerve Membrane. J. Int. Fuzzy Sys. 18, 465–475 (2007)
22. Koza, J.R., Bennett III, F.H., Andre, D., Keane, M.A., Dunlap, F.: Automated Synthesis of Analog Electrical Circuits by Means of Genetic Programming. IEEE. Trans. Evol. Comput. 1, 109–128 (1997)
23. Lapicque, L.: Recherches quantitatives sur l'excitation électrique des nerfs traitée comme une polarisation. J. Physiol. Pathol. Gen. 9, 620–635 (1907)
24. Lindsay, R.K., Buchanan, B.G., Feigenbaum, E.A., Lederberg, J.: Applications of Artificial Intelligence for Organic Chemistry: The DENDRAL Project. McGraw-Hill, New York (1980)
25. Lockery, S.R., Wittenberg, G., Kristan, W.B., Cottrell, G.W.: Function of Identified Interneurons in the Leech Elucidated Using Neural Networks Trained by Back-Propagation. Nature 340, 468–471 (1989)
26. Mattiussi, C., Floreano, D.: Analog Genetic Encoding for the Evolution of Circuits and Networks. IEEE Trans. Evol. Comp. 11, 596–607 (2007)
27. Menon, V., Spruston, N., Kath, W.L.: A State-Mutating Genetic Algorithm to Design Ion-Channel Models. PNAS 106, 16829–16834 (2009)
28. NGSpice Circuit Simulator, `http://ngspice.sourceforge.net`
29. Noble, D.: Computational Models of the Heart and Their Use in Assessing the Actions of Drugs. J. Pharm. Sci. 107, 107–117 (2008)
30. Schmidt, M., Lipson, H.: Distilling Free-Form Natural Laws from Experimental Data. Science 324, 81–85 (2009)
31. Sicard, G., Bouvier, G., Fristot, V., Lelah, A.: An Adaptive Bio-Inspired Analog Silicon Retina. In: Proc. 25th Eur. Solid-State Cir. Conf., pp. 306–309 (1999)
32. Simoni, M.F., Cymbalyuk, G.S., Sorensen, M.E., Calabrese, R.L., DeWeerth, S.P.: A Multiconductance Silicon Neuron with Biologically Matched Dynamics. IEEE Trans. Biom. Eng. 51, 342–354 (2004)
33. Smith, L.S.: Neuromorphic Systems: Past, Present and Future. Adv. Exp. Med. Biol. 657, 167–182 (2010)
34. Stanley, K.O., Miikkulainen, R.: Evolving Neural Networks Through Augmenting Topologies. Evol. Comp. 10, 99–127 (2002)
35. Torresen, J.: A Scalable Approach to Evolvable Hardware. Genet. Prog. Evol. Mach. 3, 259–282 (2002)

Appendix: Circuit Parameters

Table 1. Components and parameter ranges used in circuit evolution

Component	Parameter range
inductor	L = 1 - 1x10^9 kH
capacitor	C = 1 - 1x10^9 fF
resistor	R = 1 - 1x10^9 kΩ
diode	D
EMF	V = 0 - 20 V
p-type MOSFET	M, length = 10 μM, width = [5, 10, 20] μM
n-type MOSFET	M, length = 10 μM, width = [5, 10, 20] μM

Table 2. Components and parameter values for the evolved potassium channel equivalent circuit

Component	Parameter value
L3	3.50x10^2 kH
M3	width = 10 μM
M4	width = 5 μM
R3	3.93x10^6 kΩ
M5	width = 10 μM
M6	width = 20 μM
L4	1.79x10^5 kH
M7	width = 5 μM
C3	1.01x10^3 fF
L5	4.58x10^5 kH
L6	3.48x10^6 kH
L7	4.38x10^2 kH
C4	2.34x10^3 fF
M8	width = 10 μM
M9	width = 5 μM
L8	1.48x10^1 kH
L9	1.34x10^4 kH
C5	3.14x10^2 fF
C6	1.90x10^1 fF
L10	1.64x10^2 kH

Table 3. Components and parameter values for the evolved sodium channel equivalent circuit

Component	Parameter value
L3	3.52x10^3 kH
M3	width = 5 μM
R3	2.16x10^6 kΩ
M4	width = 10 μM
M5	width = 10 μM
C3	7.83x10^1 fF
R4	5.93x10^7 kΩ
C4	3.24x10^3 fF
M6	width = 5 μM
C5	7.07x10^8 fF
C6	4.03x10^1 fF
L4	2.21 kH
L5	2.76x10^4 kH
L6	3.48 kH